Aalborg Universitet

# Analysis of Outage Latency and Throughput Performance in Industrial Factory 5G TDD Deployments

Esswie, Ali Abdelmawgood Ali Ali; Pedersen, Klaus Ingemann

*Published in:*
2021 IEEE 93rd Vehicular Technology Conference (VTC2021)

*Publication date:*
2020

# Analysis of Outage Latency and Throughput Performance in Industrial Factory 5G TDD Deployments

Ali A. Esswie[1,2], and Klaus I. Pedersen[1,2]
[1]Nokia Bell-Labs, Aalborg, Denmark
[2]Department of Electronic Systems, Aalborg University, Denmark

*Abstract*—**The fifth generation (5G) new radio supports a diversity of network deployments. The industrial factory (InF) wireless automation use cases are emerging and drawing an increasing attention of the 5G new radio standardization groups. Therefore, in this paper, we propose a service-aware time division duplexing (TDD) frame selection framework for multi-traffic deployments. We evaluate the performance of the InF network deployments with the state-of-the-art 3GPP modeling assumptions. In particular, we consider the dynamic TDD mode along with optimized uplink power control settings. Multi-traffic coexistence scenarios are also incorporated such that quality of service (QoS) aware dynamic user scheduling and TDD link selection are introduced. Extensive system level simulations are performed in order to evaluate the performance of the proposed solutions, where the proposed QoS-aware scheme shows 68% URLLC outage latency reduction compared to the QoS-unaware solutions. Finally, the paper offers insightful conclusions and design recommendations on the TDD radio frame selection, uplink power control settings and the best QoS-coexistence practices, in order to achieve a decent URLLC outage latency performance in the state-of-the-art InF deployments.**

*Index Terms*— **Dynamic TDD; Indoor factory automation (InF); URLLC; eMBB; Cross link interference (CLI); 5G.**

## I. Introduction

The 5G new radio (5G-NR) supports multiple service classes such as the ultra-reliable and low latency communications (URLLC), and the enhanced mobile broadband (eMBB) [1]. The URLLC services require stringent radio and reliability targets, i.e., one way radio latency of 1 ms with 99.999% success probability, where the eMBB applications demand extreme data rates [2, 3]. The indoor factory automation (InF) [4, 5] use cases are emerging where the 5G-NR cellular communications are envisioned to replace the Ethernet-based interconnections. The early 5G commercial roll-outs are expected over the unpaired spectrum due to the available large free bandwidth [6, 7]. Therefore, the time division duplexing (TDD) is vital for the 5G success. For TDD deployments, base-stations (BSs) are able to dynamically change their respective radio frame configurations in order to meet the time-varying traffic demands.

Although dynamic TDD systems offer greater flexibility of the network resources in line with the directional traffic demands, the stringent URLLC latency and reliability targets are highly challenging in those networks [8]. This is attributed to: (a) the non-concurrent availability of the downlink (DL) and uplink (UL) transmission opportunities, and (b) the additional cross link interference (CLI) of BSs and user-equipment's (UEs) with concurrent opposite transmission links.

The achievable URLLC outage performance has been widely investigated for the indoor deployments [9-11], where the indoor office deployments are mainly considered. Although, to the best of our knowledge, there is a lack of prior art of the URLLC performance analysis in the InF dynamic TDD deployments and with the corresponding channel modeling and design assumptions. Furthermore, in [12], authors investigate the achievable radio outage latency in the time-sensitive communications, where a tighter synchronization and on-time delivery of packets are considered. In TDD deployments, The structure of the DL and UL link switching of the TDD radio frame and the BS-BS CLI have been proved to have a dominating impact on the URLLC outage radio latency [8]. Therefore, a diversity of inter-BS TDD radio frame coordination schemes are introduced in the open literature. In [13-15], coordinated DL beam-forming and receiver design are proposed in order to isolate the subspace of the BS-BS CLI in the spatial domain from the useful signal subspace. Moreover, smarter dynamic UE scheduling and optimized power control [16] are essential to control the network CLI. Those schemes typically require an inter-BS coordination signaling overhead, e.g., for exchanging the UE-specific allocation information.

Opportunistic TDD frame coordination schemes are also developed in order to partially or fully avoid the network CLI with simpler processing requirements and less coordination overhead. In [17], a set of TDD system optimizations, such as hybrid frame design and slot-aware dynamic UE scheduling, is combined in order to offer CLI-free channels for the UEs of the worst channel conditions. Furthermore, a semi-static TDD adaptation algorithm [18] is proposed to avoid the network CLI while offering a semi-static dynamicity of the network TDD radio frame to traffic demands. Finally, a reinforcement-learning (RL) based TDD frame optimization scheme [19] has been proposed to autonomously optimize the BS-specific TDD frame selection in a distributed manner, where the achievable learning gain offers a considerable URLLC performance improvement compared to reactive TDD adaptation schemes. Therein, two learning instances have been defined. The first learning instance estimates the best DL to UL symbol ratio to adopt during a radio frame where the second learning network seeks the best corresponding symbol placement across the frame such that the latency statistics are minimized.

In this paper, we propose a QoS-aware TDD system framework for emerging InF TDD deployments. This includes service-aware dynamic UE scheduling, TDD radio frame selection criterion. We comprehensively evaluate the achievable URLLC outage latency performance within such deployments, in combination with the eMBB services. First, we investigate the impact of the UL power control setting and CLI on the URLLC outage performance. Secondly, joint URLLC and eMBB QoS coexistence scenarios are considered. QoS-aware TDD link selection and dynamic UE scheduling are incorporated to balance among the feasibility of a decent URLLC outage latency performance and the achievable eMBB capacity. Finally, we adopt an RL based solution to dynamically optimize the selection of the BS-specific TDD frame configuration for different load regions. The presented performance evaluations are obtained through extensive system level simulations where the latest 3GPP modeling guidelines are followed. The paper offers insightful recommendations of the optimized TDD system design aspects for the InF deployments to fulfill the URLLC stringent targets.

This paper is organized as follows. Section II introduces the system modeling. Section III presents the considered QoS-aware dynamic user scheduling and TDD link selection strategy. Section IV discusses the simulation methodology and the major performance evaluation of the proposed solution. Finally, conclusions are drawn in Section VI.

## II. System Model

We consider an InF TDD network with $C$ cells, each is equipped with $N$ antennas. As depicted by Fig. 1, the network deployment follows the 3GPP modeling guidelines for InF networks [4, 5]. There are $K = K^{\text{dl}} + K^{\text{ul}}$ uniformly-distributed UEs per cell, where $K^{\text{dl}}$ and $K^{\text{ul}}$ imply the number of the DL and UL UEs per cell. Each UE is equipped with $M$ antennas, and is assumed to request both DL and UL transmissions, respectively. The URLLC service is modeled with the FTP3 traffic model [20], where the DL and UL URLLC packets are of a finite size $f^{dl}$ and $f^{ul}$ bits, respectively. URLLC packets arrive at the transmitter according to a Poisson Arrival Process with mean packet arrival rates of $\lambda^{\text{dl}}$ and $\lambda^{\text{ul}}$, in the DL and UL directions, respectively. Therefore, the offered URLLC load per cell in the DL direction is calculated by: $\Omega^{\text{dl}} = K^{\text{dl}} \times f^{dl} \times \lambda^{\text{dl}}$, and in the corresponding UL direction as: $\Omega^{\text{ul}} = K^{\text{ul}} \times f^{ul} \times \lambda^{\text{ul}}$. The total offered URLLC load is expressed as: $\Omega = \Omega^{\text{dl}} + \Omega^{\text{ul}}$. In this paper, we also assume the eMBB-URLLC coexistence scenarios solely in the DL direction, where $k^{\text{dl}}_{\text{eMBB}} \subset K^{\text{dl}}$. The eMBB traffic is modeled by a constant bit rate (CBR) per each eMBB UE [21], i.e., emulates a broadband video streaming service. Specifically, it implies finite-size eMBB packets $\rho -$ bits which arrive at the transmitter with a constant arrival rate in time. For those scenarios, the total offered load in DL direction is calculated as: $\Omega^{\text{dl}} = \left(\Omega^{\text{dl}}\right)^{\text{eMBB}} + \left(\Omega^{\text{dl}}\right)^{\text{urllc}}$, where $\left(\Omega^{\text{dl}}\right)^{\text{eMBB}}$ is the eMBB offered load.

The UEs are dynamically multiplexed using the orthogonal frequency division multiple access (OFDMA). In line with the 3GPP assumptions for URLLC, we adopt a sub-carrier spacing (SCS) of 30 kHz with a physical resource block (PRB) of twelve consecutive SCSs. We assume a short transmission time interval (TTI) of 4 OFDM symbol duration for both URLLC and eMBB transmissions. Before the start of each radio frame (10 ms), each BS decides the structure of the selected slot formats within the radio frame, where there is a guard symbol between each DL and UL TTI transition to compensate for the channel propagation delay.

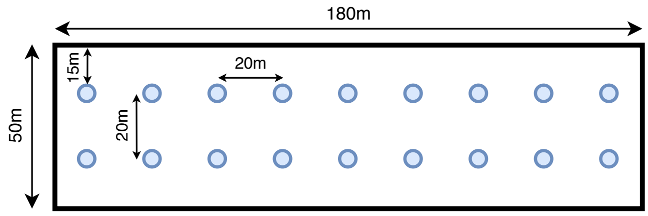


Fig. 1. System model: InF network deployment.

In line with the system modeling assumptions in [19], we explicitly consider the major functionalists of the 5G NR PHY and MAC layers. In the DL direction, arriving packets are first processed, and are buffered towards the first available DL TTI of the current TDD radio frame. The DL UEs are dynamically scheduled using the adopted MAC scheduler. The DL packets are subject to a further processing delay at the UE-side. In case the DL packets are not successfully decoded, UEs trigger a HARQ negative ACK (NACK) during the first available UL TTI. Subsequently, the serving BSs re-transmit the failed DL packets during the next available DL transmission opportunity. We adopt dynamic link adaptation in the DL direction, based on periodic reporting of the channel quality indications (CQIs) to select the best corresponding modulation and coding scheme (MCS) to achieve the target block error rate (BLER).

In the UL direction, in line with [22], we consider the configured grant (CG) transmission with a fixed MCS per UE. With CG, the arriving UL packets at the UE-side side are immediately prepared for UL transmissions during the first available UL TTI. This removes the delay for transmitting the scheduling request until receiving the corresponding scheduling grant. All CG-based UL transmissions include a robust preamble such that the BS is able to distinguish from which UEs the UL transmission is initiated. The CG UL configurations are set such that all active UL UEs transmit over a randomly selected sub-band, of one quarter of the carrier bandwidth, with a predefined MCS level of QPSK rate 1/2. This setting allows for transmitting one full URLLC packet in a single shot without segmentation.

The UL transmission power is configured as

$$\Sigma\,[dBm] = \min\left\{\Sigma_{\text{max}},\ P0 + 10\log_{10}(\wp) + \alpha\eth\right\}, \qquad (1)$$

where $\Sigma_{\text{max}}$ is the maximum UE transmit power, $P0$ is the power spectral density, $\wp$ is the number of granted UL PRBs, $\alpha$ and $\eth$ are the path-loss compensation factor and path-loss. As CG transmissions from different UEs can be transmitted over overlapping resources, those are subject to intra-cell interference. In case the BS fails to decode UL transmissions from different UL UEs, the BS triggers a re-transmission request during the first available DL TTI with a dedicated scheduling grant for the UE. Correspondingly, the UL UE initiates a packet re-transmission using the same MCS and bandwidth configuration as the first UL transmission, with a 3 dB transmission power boost to improve the decoding probability of the HARQ re-transmission [22].

## III. Key Factors Impacting The URLLC Performance in InF Deployments

In the following subsections, we show the critical 5G NR system design aspects impacting the achievable URLLC outage performance within the emerging InF TDD deployments. Those span the optimization of the UL power control settings, dynamic UE scheduling, and the TDD link selection framework, respectively.

### A. QoS-aware TDD Radio Frame Selection

In dynamic TDD networks, BSs independently select the radio frame structures, in terms of the number of the DL and UL transmission opportunities across the frame duration, that best meet their respective traffic needs. Therefore, BSs continuously monitor their offered traffic demands in the DL and UL directions. We formulate the relative buffered traffic ratio $\mu_{[t,c]}(\varsigma)$ at the $\varsigma^{th}$ slot of the radio frame, $\varsigma = 1, 2, \ldots, \xi$, and $\xi$ is the number of slots per the radio frame as

$$\mu_{[t,c]}(\varsigma) = \frac{Z^{\text{dl}}_{[t,c]}(\varsigma)}{Z^{\text{dl}}_{[t,c]}(\varsigma) + (1/\iota)\, Z^{\text{ul}}_{[t,c]}(\varsigma)}, \tag{2}$$

where $Z^{\text{dl}}_{[t,c]}(\varsigma)$ and $(1/\iota)\, Z^{\text{ul}}_{[t,c]}(\varsigma)$ denote the total DL and UL buffered traffic size of the $\varsigma^{th}$ slot during the current frame, and $\iota$ implies the first-transmission average UL BLER at the BS side. The latter is linearly averaged across all UL transmissions and updated using a sliding window per UE. The intuition of such formulation is derived by the fact that the BS has different knowledge of the $Z^{\text{dl}}_{[t,c]}(\varsigma)$ and $Z^{\text{ul}}_{[t,c]}(\varsigma)$ information. In particular, the knowledge of the $Z^{\text{dl}}_{[t,c]}(\varsigma)$ is available at the BS. However, in the UL direction, the buffered first UL transmission size per UE $Z^{\text{ul}}_{[t,c]}(\varsigma)$ is not immediately accessible at the BS until it is received at the BS side. Therefore, the term $(1/\iota)\, Z^{\text{ul}}_{[t,c]}(\varsigma)$ is adopted to reflect the actual offered UL traffic size, i.e., equivalent to $Z^{\text{dl}}_{[t,c]}(\varsigma)$ in the DL direction.

For multi-traffic deployments with joint URLLC-eMBB, the terms $Z^{\text{dl}}_{[t,c]}(\varsigma)$ and $(1/\iota)\, Z^{\text{ul}}_{[t,c]}(\varsigma)$ represent the aggregate URLLC-eMBB buffered traffic sizes in the DL and UL directions, respectively. As the eMBB traffic demand is typically much larger than of the corresponding URLLC, the buffer ratio in (2) and the selection of the TDD frame are both dominated by the eMBB traffic statistics instead. This could be problematic to achieve a decent URLLC outage latency due to the additional URLLC packet buffering, i.e., due to the selection of a radio frame configuration that does mainly satisfy with the buffered URLLC traffic. Therefore, we adopt a QoS-aware TDD link selection criterion such as the buffered traffic statistic in (2) is biased towards the URLLC QoS as follows

$$\begin{array}{l} Z^{\text{dl/ul}}_{[t,c]}(\varsigma) \rightarrow \left(Z^{\text{dl/ul}}_{[t,c]}(\varsigma)\right)^{\text{urllc}}, \text{URLLC-only} \\ Z^{\text{dl/ul}}_{[t,c]}(\varsigma) \rightarrow \left(Z^{\text{dl/ul}}_{[t,c]}(\varsigma)\right)^{\text{eMBB}}, \text{eMBB-only} \end{array}, \tag{3}$$

where $\left(Z^{\text{dl}}_{[t,c]}(\varsigma)\right)^{\text{urllc}}$, $\left(Z^{\text{dl}}_{[t,c]}(\varsigma)\right)^{\text{eMBB}}$, $\left(1/\iota Z^{\text{ul}}_{[t,c]}(\varsigma)\right)^{\text{urllc}}$, and $\left(1/\iota Z^{\text{ul}}_{[t,c]}(\varsigma)\right)^{\text{eMBB}}$ are the aggregate DL and UL buffered traffic sizes for the URLLC and eMBB UEs, respectively. The instantaneous buffered traffic ratios $\mu_{[t,c]}(\varsigma)$ are averaged over the duration of the TDD radio frame given as

$$\overline{\mu}_{[t,c]} = \frac{1}{\xi} \sum_{\varsigma=1}^{\xi} \mu_{[t,c]}(\varsigma), \tag{4}$$

where $\overline{\mu}_{[t,c]}$ is the average traffic ratio of the current radio frame. The traffic ratio $\overline{\mu}_{[t,c]} \rightarrow [0, 1]$ implies the combined buffering performance of the DL and UL traffic size. For example, $\overline{\mu}_{[t,c]} = 0.1$ implies that the buffered UL traffic is 9x times the corresponding DL traffic. Therefore, the corresponding BS shall select a TDD radio frame with 90% of time allocation to the UL transmission opportunities, assuming a similar UL and DL spectral efficiency. The DL and UL symbols of the selected radio frames are evenly distributed in terms of 4 OFDM symbol blocks, following the adopted DL-to-UL symbol ratio.

### B. QoS-aware Dynamic UE Scheduling

To highlight the impact of the UE scheduler, we adopt two frameworks of the multi-QoS dynamic UE schedulers. First, we consider the well-known weighted proportional fair (PF) criterion [23] to dynamically schedule different URLLC and eMBB UEs in the time and frequency domains. UEs are sorted in the time domain such as the URLLC UEs are always given a higher priority than the eMBB UEs, i.e., URLLC UEs are given a higher weight in the PF criterion. Therefore, the higher PF weight of the URLLC UEs aims to always schedule the active URLLC UEs before the respective eMBB UEs in the time domain. Thereafter, active URLLC and eMBB UEs are both scheduled based on the PF criterion in the frequency domain. That is, according to their achievable instantaneous throughput relative to the total received capacity. This way, the scheduling fairness is always guaranteed in the frequency domain among each set of the URLLC and eMBB UEs, respectively. The main drawback of such scheduling framework is that the URLLC latency statistics are not considered in the scheduling criterion, and therefore, it could lead to a degraded URLLC outage latency performance.

Secondly, we adopt the scheduling framework introduced in [24]. Instead of the throughput-based PF scheduling criterion, the head of line delay (HoLD) is the basic scheduling criterion. The HoLD per packet per UE is defined as the time from the DL packet arrives at the transmitter end until it is successfully decoded at the intended receiver end. The scheduler always prioritizes an immediate scheduling for the URLLC UEs with the largest HoLD statistics while requiring the least packet segmentation. The intuition is that the scheduler seeks to minimize the probability of the URLLC packet segmentation probability, therefore, reducing the URLLC outage latency. In case packet segmentation is not avoidable due to the resource shortage, the scheduler seeks to segment a single URLLC packet that leads to the minimum control overhead per TTI, hence, leaving more resource for data transmissions. In joint URLLC-eMBB deployments, such scheduler is proved to offer considerable eMBB capacity, due to the faster transmissions of the concurrent URLLC packets, therefore, leaving more resources for the corresponding eMBB traffic.

## IV. Performance Evaluation

### A. Simulation Methodology

We adopt a highly-detailed system level simulations to evaluate the performance of the proposed solutions. The main set of the simulation parameters is listed in Table I. We adopt the dense clutter - high BS propagation model of the InF deployments [4, 5], where the BSs are elevated as compared to active UEs. The simulator used for the system level evaluations has a timing resolution of a single OFDM symbol and includes the main functionalities of the 5G NR protocol stack. The simulator is validated via calibration exercises, where baseline statistics for predefined simulation scenarios are reported and compared between the various 3GPP partners [25]. For each radio frame of 10 ms, the BSs select the radio frame configurations which best suit their current DL and UL traffic demand. During the DL TTIs, UEs are dynamically scheduled using either the PF or min-HoLD [24] criterion. During the UL TTIs, UEs transmit their UL packets using the CG UL following the settings presented in Section II. For DL/UL packets, the signal to interference noise ratios (SINR) of the granted sub-carriers are calculated using the linear minimum mean square error interference rejection and combining receiver (L-MMSE-IRC). Those are combined using the mean mutual information per coded bit (MMIB) mapping [26] in order to estimate the effective SINR point. Based on the effective SINR, the corresponding error probability is calculated using look-up tables, obtained from extensive link level simulations, considering the received effective SINR and the adopted MCS.

Table I
Simulation parameters.

| Parameter | Value |
|---|---|
| Environment | 3GPP-InF, one cluster, 18 cells |
| UL/DL channel bandwidth | 20 MHz, SCS = 30 KHz, TDD |
| Channel model | InF-DH (dense clutter and high BS) [5] |
| BS and UE transmit power | BS: 30 dBm, UE: 23dBm |
| Carrier frequency | 3.5 GHz |
| BS and UE heights | BS: 10m, UE: 1.5m |
| Antenna setup | $N = 4$ , $M = 4$ |
| Average UEs per cell | $K^{\text{dl}} = K^{\text{ul}} =$ 8-16 |
| TTI configuration | 4-OFDM symbols |
| URLLC Traffic model | FTP3, $f^{dl}$ = $f^{ul}$ = 256 bits<br>$\lambda^{\text{dl}}$ = 50 pkts/sec<br>$\lambda^{\text{ul}}$ = 50 pkts/sec |
| eMBB Traffic model | CBR, $\rho =$ 16k bits, rate/UE = 0.5 Mbps |
| DL scheduling | PF, min-HoLD [24] |
| UL scheduling | CG, QPSK1/2, $P0$= -61 dBm, $\alpha$= 1 |
| Processing time | PDSCH prep. delay: 2.5-OFDM symbols<br>PUSCH prep. delay: 5.5-OFDM symbols<br>PDSCH decoding : 4.5-OFDM symbols<br>PUSCH decoding: 5.5-OFDM symbols |
| DL/UL receiver | L-MMSE-IRC |
| TDD frame | 10 ms |

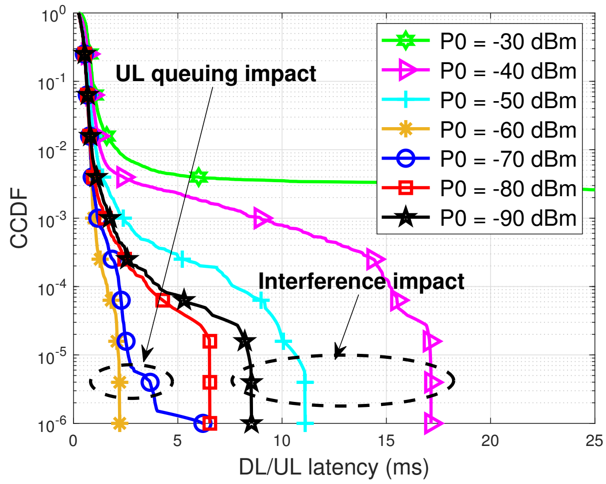


Fig. 2. Achievable URLLC latency with dynamic TDD for different $P0$.

### B. Performance Results

The UL power control settings have a vital impact on the overall URLLC performance. Fig. 2 presents the complementary cumulative distribution function (CCDF) of the achievable URLLC latency with different UL power control settings, i.e., for several $P0$ configurations. As can be clearly observed, with $P0 = -90$ to $-60$ dBm, a decent URLLC outage latency performance is obtained. Herein, the majority of the UL UEs transmit their UL packets with a lower transmission power. Therefore, the inter-cell interference is controlled while the UL packet queuing delay dominates the achievable URLLC outage latency. With very high $P0 = -40$ to $-30$ dBm, the majority of the UL UEs transmit their payload with the maximum permissible transmission power, resulting in a significant increase of the inter-cell interference. Hence, the interference starts to dominate the URLLC outage latency where the packets require multiple HARQ re-transmission combing attempts before a successful decode, leading to a highly degraded URLLC outage latency performance. Based on the obtained URLLC performance in Fig. 2, we adopt $P0 = -61$ dBm for the rest of the results in order to achieve the best possible URLLC outage latency.

Fig. 3 depicts the CCDF of the achievable combined DL/UL URLLC latency for different offered loads. For the low load region with $\Omega = 0.5$ Mbps, the URLLC target is achieved, i.e., a fully dynamic TDD satisfies the URLLC outage latency target of 1 ms. This is mainly attributed to the low CLI intensity and the smaller queuing delays under such very low offered load. For higher offered loads of $\Omega = 3$ Mbps, the achievable URLLC outage latency inflicts a clear increase due to the packet queuing delay. Moreover, the CLI is shown to have a minor effect on the achievable URLLC latency for the low and moderate offered load levels.

Next, we investigate the URLLC and eMBB coexistence performance under different scheduling policies. Fig. 4 depicts

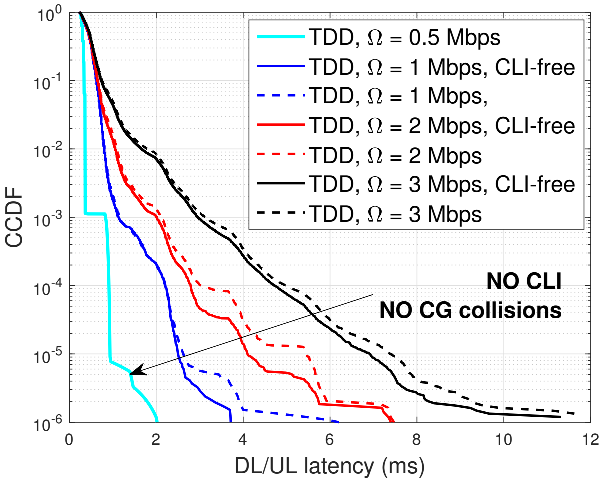


Fig. 3. Achievable URLLC latency with dynamic TDD for different loads.

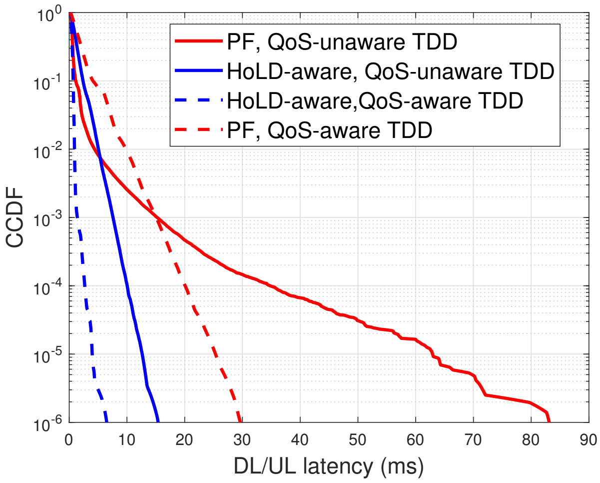


Fig. 4. Achievable URLLC latency for different dynamic UE scheduling and TDD link selection.

the CCDF of the achievable URLLC latency, where $\Omega = 2$ Mbps, and the eMBB traffic is only incorporated in the DL directions with 3 eMBB UEs per cell, each has a CBR of 0.5 Mbps. The throughput-based PF dynamic UE scheduler fails to achieve a decent URLLC outage compared to the HoLD-aware scheduler [24]. This is mainly because the latter considers the latency statistics of pending URLLC UEs in the scheduling criterion. It seeks to schedule the URLLC UEs with the largest HoLD statistics while reducing the probability of the packet segmentation. Furthermore, adopting a QoS-aware TDD link selection criterion tends to significantly improve the achievable URLLC performance, i.e., 68% outage latency reduction compared to the URLLC QoS-unaware TDD selection criterion. This is attributed to the fact that with the QoS-aware TDD link selection, the selection of the TDD frame configuration is dictated by the URLLC offered traffic size, instead of the aggregate URLLC/eMBB traffic, reducing the TDD link switching delay of the urgent URLLC packets.

Fig. 5 shows the empirical CDF (ECDF) of the achievable

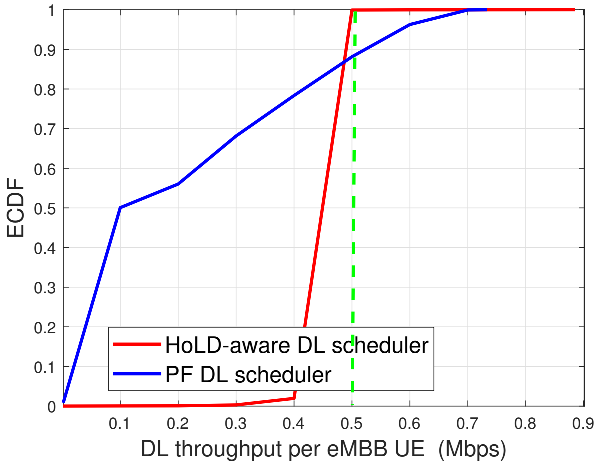


Fig. 5. Achievable eMBB CBR rate for URLLC-eMBB coexistence.

throughput per eMBB UE. The source CBR rate is pre-configured as 0.5 Mbps per UE. As depicted, the achievable eMBB throughput with the HoLD-aware scheduler approaches the source CBR rate, while significantly outperforming the case with the PF scheduler. This is mainly because: (1) the URLLC transmissions are scheduled in a faster basis while the URLLC packet segmentation is reduced, and (2) in the frequency domain, URLLC packets are scheduled based on the throughput-to-average criterion which further minimizes the required total number of PRBs to allocate the active URLLC UEs. The HoLD-aware scheduler attempts to avoid the URLLC packet segmentation, resulting from the insufficiently available free resources. In case this is not possible, the scheduler seeks to inflict segmentation of the URLLC packets that result in the lowest possible control overhead. Therefore, it leaves more resources for the respective eMBB traffic, and accordingly, achieving a highly optimized eMBB capacity compared to the case with the PF scheduler.

Finally, we investigate the potential of the RL-based TDD frame selection solution [19] compared to the non-RL based TDD frame selection schemes, i.e., reactive TDD, where only the URLLC traffic is considered. Fig. 6 depicts the achievable URLLC latency performance when such learning approach is adopted for different load regions. As can be observed, at the low load region, both the RL-based TDD and reactive dynamic TDD schemes offer a similar URLLC outage performance. This is mainly due to the low resource utilization, thus, adopting predefined random UL/DL allocations during the selected TDD frame, in line with the buffered traffic ratio, is sufficient. At the high load region, the resource utilization increases, introducing additional queuing delays for urgent URLLC packets in both the DL and UL directions. Therefore, due to the smarter and latency-aware adaptation of the RL-based TDD solution, the TDD learning approach obviously outperforms the basic dynamic TDD scheme.

## V. Concluding Remarks

We have evaluated the achievable URLLC performance for the emerging indoor factory automation 5G network deployments. We have analyzed the state-of-the-art dynamic

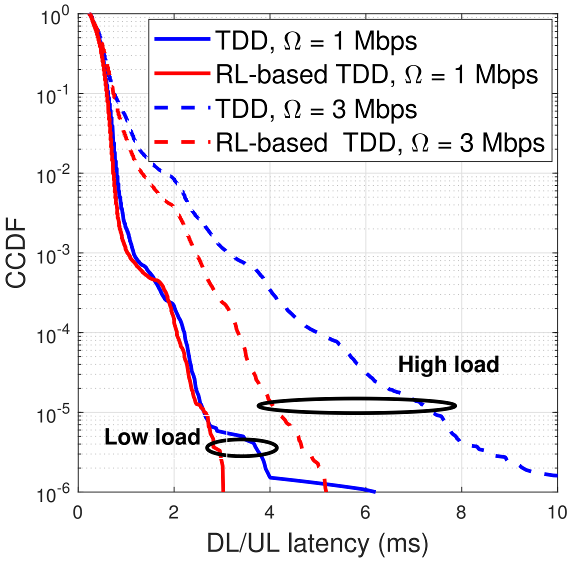


Fig. 6. Achievable URLLC latency with the reinforcement learning approach.

TDD duplexing scheme with optimized uplink power control settings. For the URLLC-eMBB coexistence scenarios, we adopt quality of service (QoS)-aware dynamic user scheduling and TDD link selection strategy, respectively. The main recommendations offered by this paper are as follows: (a) for the indoor factory deployments, the CLI is not a major critical performance bottleneck as the case with the macro networks, due to the InF prorogation conditions, and the smaller difference between the uplink and downlink transmission power, (2) the optimization of the uplink control settings has a vital impact on the achievable URLLC outage performance. Unoptimized uplink power control configurations could either lead to a further uplink queuing delay or a significantly higher inter-cell same and cross-link interference. Therefore, we recommend setting $P0 = -61$ dBm within the indoor factory deployments to achieve the best possible URLLC outage latency, (3) within multi-QoS coexistence scenarios, latency-aware dynamic user scheduling and TDD frame selection strategies are vital to achieve a decent URLLC latency performance, and (4) reinforcement learning (RL) based TDD frame adaptation is effective in achieving a decent URLLC outage latency within InF deployments, through the dynamic selection of the number and placement of the downlink and uplink transmission opportunities across the TDD radio frame which best reduces the overall radio latency. However, it requires a careful modeling of the learning objectives, inputs, and outputs.

## VI. Acknowledgments

This work is partly funded by the Innovation Fund Denmark – File: 7038-00009B. The authors would like to acknowledge the contributions of their colleagues in the project.

## References

[1] *Framework and Overall Objectives of the Future Development of IMT for 2020 and Beyond*, ITU-R M.2083-0, International Telecommunication Union (ITU), Feb. 2015.

[2] *Service requirements for the 5G system*; Stage-1 (Release 16), 3GPP, TS 22.261, V16.6.0, Dec. 2018.

[3] M. Bennis, M. Debbah and H. V. Poor, "Ultrareliable and low-latency wireless communication: tail, risk, and scale," *Proc. of the IEEE*, vol. 106, no. 10, pp. 1834-1853, Oct. 2018.

[4] *Service requirements for cyber-physical control applications in vertical domains*; Stage-1 (Release 17), 3GPP, TS 22.104, V17.3.0, July 2020.

[5] *Study on channel model for frequencies from 0.5 to 100 GHz*; Release 16, 3GPP, TR 38.901, V16.1.0, Dec. 2019.

[6] J. Lee et al., "Spectrum for 5G: global status, challenges, and enabling techs," *IEEE Commun. Mag.*, vol. 56, no. 3, pp. 12-18, Mar. 2018.

[7] K. I. Pedersen, G. Berardinelli, F. Frederiksen and P. Mogensen, "A flexible 5G wide area solution for TDD with asymmetric link operation," *IEEE Wireless Commun.*, vol. 24, no. 2, pp. 122-128, April 2017.

[8] Ali A. Esswie, and K.I. Pedersen, "On the ultra-reliable and low-latency communications in flexible TDD/FDD 5G networks," *in Proc. IEEE CCNC,* Las Vegas, Jan. 2020.

[9] L. Wang and H. Zhang, "Analysis of joint scheduling and power control for predictable URLLC in industrial wireless networks," *in Proc. IEEE ICII* , Orlando, FL, USA, 2019, pp. 160-169.

[10] M. Alonzo, P. Baracca, S. R. Khosravirad and S. Buzzi, "URLLC for factory automation: an extensive throughput-reliability analysis of D-MIMO," *in Proc. IEEE WSA,* Hamburg, Germany, 2020, pp. 1-6.

[11] V. Hytönen, Z. Li, B. Soret and V. Nurmela, "Coordinated multi-cell resource allocation for 5G ultra-reliable low latency communications," *in Proc. IEEE EuCNC*, Oulu, 2017, pp. 1-5.

[12] R. B. Abreu, G. Pocovi, T. H. Jacobsen, M. Centenaro, K. I. Pedersen and T. E. Kolding, "Scheduling enhancements and performance evaluation of downlink 5G time-sensitive communications," *IEEE Access*, vol. 8, pp. 128106-128115, 2020.

[13] Z. Huo, N. Ma and B. Liu, "Joint user scheduling and transceiver design for cross-link interference suppression in MU-MIMO dynamic TDD systems," *in Proc. IEEE ICCC,* Chengdu, Dec. 2017, pp. 962-967.

[14] A. Łukowa and V. Venkatasubramanian, "Performance of strong interference cancellation in flexible UL/DL TDD systems using coordinated muting, scheduling and rate allocation," *in Proc. IEEE WCNC*, Doha, April 2016, pp. 1-7.

[15] Ali A. Esswie, and K.I. Pedersen, "Cross link interference suppression by orthogonal projector in 5G dynamic-TDD URLLC systems," *in Proc. IEEE WCNC,* April 2020.

[16] A. Łukowa and V. Venkatasubramanian, "Coordinated user scheduling in 5G dynamic TDD systems with beamforming," *in Proc. IEEE PIMRC*, Bologna, Sep. 2018, pp. 596-597.

[17] Ali A. Esswie, K.I. Pedersen, and P. Mogensen, "Quasi-dynamic frame coordination for ultra- reliability and low-latency in 5G TDD systems," *in Proc. IEEE ICC*, Shanghai, China, May 2019, pp. 1-6.

[18] Ali A. Esswie, K.I. Pedersen, and P. Mogensen, "Semi-static radio frame configuration for URLLC deployments in 5G macro TDD networks," *in Proc. IEEE WCNC,* April 2020.

[19] A. A. Esswie, K. I. Pedersen, and P. Mogensen, "Online radio pattern optimization based on dual reinforcement-learning approach for 5G URLLC networks," *IEEE Access*, 2020.

[20] *Study on new radio access technology physical layer aspects*; Release 14, V14.2.0, TR 38.802, 3GPP, Sep. 2017.

[21] Tong Shan, O. Yang and Genzao Zhang, "Scheduling jittered CBR traffic in broadband wireless access systems," *in Proc. IEEE ICC*, Anchorage, AK, 2003, pp. 22-26.

[22] T. Jacobsen, R. Abreu, G. Berardinelli, K. Pedersen, I. Z. Kovács and P. Mogensen, "Joint resource configuration and MCS selection scheme for uplink grant-free URLLC," *in Proc. Globecom*, Abu Dhabi, United Arab Emirates, Dec. 2018, pp. 1-6.

[23] M. K. Müller, S. Schwarz and M. Rupp, "QoS investigation of proportional fair scheduling in LTE networks," *in Proc. IEEE IFIP (WD)*, Valencia, 2013, pp. 1-4.

[24] A. Karimi, K. I. Pedersen, N. H. Mahmood, G. Pocovi and P. Mogensen, "Efficient low complexity packet scheduling algorithm for mixed URLLC and eMBB traffic in 5G," *in Proc. IEEE VTC-Spring*, Kuala Lumpur, Malaysia, 2019, pp. 1-6.

[25] *Study on physical layer enhancements for NR ultra-reliable and low latency case (URLLC)*, Release 16, TR 38.824, 3GPP, Mar. 2019.

[26] D. G. Popescu, M. Varga and V. Bota, "Comparison between measured and computed values of the mean mutual information per coded bits in OFDM based wireless transmissions," *in Proc. IEEE Conference on Telecommunications and Signal Processing (TSP)*, Rome, July 2013, pp. 380-384.